ARTICLE

fib WILEY

Comparative study of probabilistic modeling approaches for chloride ingress in concrete structures with macro-cracks

Annika Lidwina Schultheiß[1,2] ⓘ　│　**Ravi A. Patel**[1,2]　│　**Michael Vogel**[1,2]　│
Frank Dehn[1,2]

[1]Institute of Building Materials and Concrete Structures (IMB), Karlsruhe Institute of Technology (KIT), Karlsruhe, Germany

[2]Materials Testing and Research Institute Karlsruhe (MPA), Karlsruhe Institute of Technology (KIT), Karlsruhe, Germany

Correspondence
Annika Lidwina Schultheiß, Karlsruhe Institute of Technology (KIT), DE-76131, Karlsruhe, Germany.
Email: annika.schultheiss@kit.edu

Abstract

Probabilistic service life analyses for assessing the risk of chloride-induced corrosion in uncracked concrete are often realized using the well-known chloride ingress model of the *fib* Model Code for Service Life Design. In practice, however, concrete includes cracks, which alter the resistance of the concrete against the chloride ingress. In the past, different approaches to account for preexisting cracks, were developed. In this study, these modeling approaches are summarized and compared in context of the probabilistic service life prognosis. Furthermore, a new approach to account for cracks by theoretically adapting the convection zone is presented. This study demonstrates that the choice of model extension to account for cracks vastly influences the prediction results and shows the limits of application of the current extensions.

KEYWORDS

chloride ingress, concrete, cracks, probabilistic service life prognosis

1 │ INTRODUCTION

Chloride-induced corrosion of reinforcing steel in concrete is known to be one of the major causes of serious deterioration of reinforced concrete structures exposed to marine environment or deicing salts during winter. In uncracked concrete, chlorides are transported mainly through diffusion and convection-diffusion, when rapid changes occur in relative humidity and temperature. Hence, for practical service life predictions chloride ingress is modeled as diffusive process and often Gauss error function (erf) based models are used to predict the chloride content as a function of concrete depth. For these models, the diffusion coefficient is the most important material input parameter. Models for an engineering service life prediction, such as one given in the *fib* Model Code for Service Life Design[1] (hereafter referred to as *fib* chloride model), are coupled with probabilistic reliability analysis. Such analyses allow to account for uncertainties associated with input variables such as material properties, environmental factors, and the geometry of the structure. The determined probability of chloride induced depassivation of the reinforcement is conservatively defined as the probability of failure, as it indicates the corrosion initiation.

In reinforced concrete structures, cracks can hardly be avoided. Cracks on the concrete surface can be caused by several factors such as shrinkage, temperature gradients, or mechanical loading.[2,3] Cracks increase the diffusion coefficient, which significantly depends on parameters such as

crack width, crack roughness, crack tortuosity, and crack path connectivity.[4] To account for cracks in chloride ingress models, the diffusion coefficient is often modified. A smeared diffusion coefficient can be determined experimentally by fitting the erf-solution to the chloride profiles in the cracked area. Alternatively, the smeared diffusion coefficient of the analytical composite media theory considers the diffusion coefficients in the crack and in the concrete proportionally to their fraction of the exposed surface area. Gérard and Marchand[5] presented this approach for traversing cracks and theoretically analyzed their influence on transport of ions in saturated concrete. Lu et al.,[6] Gao et al.,[7] and Park et al.,[8] adapted this model and used it also for V-shaped cracks caused by bending.

Crack influence factors (CIFs), give the ratio of the smeared diffusion coefficient to the diffusion coefficient in uncracked concrete. Both diffusion coefficients can be derived by the fitting of experimental determined chloride profiles. The diffusion coefficient used in the erf-solution is then multiplied with the CIF to account for the presence of cracks. Several researchers have determined CIFs as a function of the crack width.[9–15]

In the literature, several studies with probabilistic reliability analyses have been carried out to account for cracks in concrete structures. The results from these studies are hardly comparable. For instance, using the CIF of Kwon et al.[12] showed for a wharf structure, that the change in crack width from 0.0 to 0.3 mm reduces the predicted service life for a probability of failure of 10% in the crack region from 84.5 years to only 13 years. Schmiedel et al.[10] determined the probability of failure of a 36 year old bridge in the uncracked and cracked zone with CIFs. In the intact concrete, the probability of failure was about 9%, whereas in the cracked area, it increased to 45% and 49% for crack widths of 0.2 and 0.3 mm, respectively. Using the composite approach, Lu et al.,[6] predicted that the service life of a bridge beam would be reduced by 12% when the effect of load-induced cracks was considered.

Different approaches to account for cracks in the erf-solution can be found in the literature. Whether these approaches will provide comparable results, when used in the *fib* chloride model, is however unclear. In practical engineering, the *fib* chloride model is widespread and therefore the application of the model extensions for this model must be evaluated. In this study, the *fib* chloride model for uncracked concrete is used as the basis for the extensions, which account for preexisting cracks. Different approaches are discussed in detail. This includes the adaption of the diffusion coefficient with the composite approach or the CIF approach and a new approach adapting the convection zone. Using the presented model extensions, a case study for the service life prediction of concrete with preexisting crack is developed. This allows the comparison of the probabilities of failure according to

the different approaches. Furthermore, a distinction between the service life of the cracked region and the whole structure is made and the different model extensions are discussed in each of these contexts. Finally, drawbacks of these model extensions are extensively discussed, and future research needs are highlighted.

2 | *fib* CHLORIDE MODEL FOR UNCRACKED CONCRETE

In uncracked concrete, it is acknowledged that diffusion is the principal mechanism beyond the near surface zone.[16] Fick's second law of diffusion is usually applied in Equation (1) with presented boundary conditions to quantify the chloride concentration $C(x,t)$ (kg/m^3 of pore solution) in the aqueous phase at a certain position and time.[1,16–20]

$$\begin{cases} \dfrac{\partial C}{\partial t} = -\dfrac{D_e}{\Theta + \dfrac{\partial C_b}{\partial C}} \dfrac{\partial^2 C}{\partial x^2} = -D_{\text{app}} \dfrac{\partial^2 C}{\partial x^2} \\ C(x,0) = 0, C(0,t) = C_s, C(\infty,t) = 0 \end{cases} \quad (1)$$

where, D_e (m^2/s) is the effective diffusion coefficient, Θ [$-$] is the porosity, $\frac{\partial C_b}{\partial C}$ [$-$] is the binding capacity of the cement-based material, C_b (kg/m^3 of paste/mortar/concrete) is the bound chloride concentration and D_{app} (m^2/s) is the apparent diffusion coefficient. Additionally to tortuosity effects, the apparent diffusion coefficient accounts for binding of chlorides, which can vary with time.[19,21] Although the model in Equation (1) simplifies the overall process of chloride transport in concrete structures, it is widely used for service life predictions.[20]

The analytical solution of Equation (1) is given in Equation (2). This solution is commonly used and referred to as erf-solution. The erf-solution assumes (1) that the domain is semi-infinite, but for $2\sqrt{D_{\text{app}}t} \ll l$, it is a good predictor for finite-width systems,[20] (2) that concrete is homogeneous in structure, (3) fully saturated, (4) that the apparent diffusion coefficient D_{app} is independent of the humidity of concrete, chloride concentration and temperature, while the binding isotherm is linear, (5) that $C(x,t=0)$ is zero, and (6) that the surface concentration C_s (wt.-% of binder) is constant.[17,18,22,23]

$$C(x,t) = C_s \left[1 - erf \left(\frac{x}{2\sqrt{D_{\text{app}} \cdot t}} \right) \right] \quad (2)$$

To take the material and environmental induced changes into D_{app}, the experimentally determined rapid chloride migration coefficient $D_{\text{RCM},0}$ (m^2/s) in the *fib* chloride model transformed to a time-dependent $D_{\text{app},c}$ (m^2/s)

according to Equation (3). The instantaneous $D_{\text{app},c}$ obtained from Equation (3) is derived from chloride profiles, which are obtained as a result of the exposure till the date of inspection. While Equation (2) still remains as the exact the analytical solution of Equation (1), in case of time dependent diffusion coefficient,[23] Equation (3) is purely an empirical extension.[17,24]

$$D_{\text{app},c} = \exp\left(b_e\left(\frac{1}{T_{\text{ref}}} - \frac{1}{T_{\text{real}}}\right)\right) D_{\text{RCM},0} \cdot k_t \left(\frac{t_0}{t}\right)^\alpha \quad (3)$$

Where b_e is a regression variable (K), T_{ref} and T_{real} are the reference and ambient temperature in (K), k_t is the transfer variable $[-]$, t_0 and t are the reference time and the target time for the prediction (years) and α is the aging exponent $[-]$.

Measured chloride profiles often show a deviation from the erf-solution in the region close to the exposed surface due to the convective process of wetting and drying.[1,25] Therefore, at the depth of the convection zone Δx (mm), a substitute surface concentration $C_{S,\Delta x}$ (wt.-% of binder) is used in the *fib* chloride model. Another empirical adjustment of the erf-solution used in the *fib* chloride model is the consideration of the initial chloride content C_0 (wt.-% of binder). Further, in context of the limit state for the service life prediction, the prediction of the chloride content at cover depth a (mm) is sufficient. Hence, Equation (2) is adapted in Reference 1 as given below:

$$C(a,t) = C_0 + (C_{S,\Delta x} - C_0)\left[1 - \text{erf}\left(\frac{a - \Delta x}{2\sqrt{D_{\text{app},c} \cdot t}}\right)\right] \quad (4)$$

For uncracked concrete, Equation (4) can be used in conjunction with the probabilistic approach to predict the service time for a threshold probability of failure p_f due to chloride-induced rebar depassivation. The same procedure can be used for the service life prediction of cracked concrete if Equation (4) or its input parameters are adapted. In both cases, the limit-state equation (Equation (5)) compares the critical chloride concentration C_{crit} (wt.-%/binder) to the actual chloride concentration at the depth of the rebar at a time of service life $C(x = a, t = t_{\text{SL}})$.

$$p_{\text{dep}} = p\{C_{\text{crit}} - C(a, t_{\text{SL}}) < 0\} < p_{f,lim}(t_{\text{SL}}) \quad (5)$$

Probabilistic reliability analyses can be easily carried out by Monte Carlo simulation with Equation (5) as limit state equation. Alternatively, the First-Order Reliability Method or the Second-Order Reliability Method can be used as a sufficient approximation. The input parameters are random variables described with appropriate distribution functions.
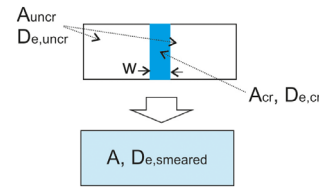

FIGURE 1 Schematic illustration of the composite approach according to Gérard and Marchand[5]

3 | EXTENSION OF THE *fib* CHLORIDE MODEL FOR CRACKED CONCRETE

To apply the *fib* chloride model, which is discussed in section 2, Equation (4) can be used by either adapting the apparent diffusion coefficient $D_{\text{app},c}$ to account for pre-existing cracks or by adapting the convection zone Δx. Both these approaches and their variations are explained in the following section and discussed in the context of the probabilistic service life analysis.

3.1 | Determination of the smeared diffusion coefficient

The smeared diffusion coefficient D_{smeared} is often used to adapt the apparent diffusion coefficient $D_{\text{app},c}$ of the *fib* chloride model. The theoretical basis of the two approaches to determine D_{smeared} are explained in the following section.

3.1.1 | Composite approach

All composite approaches to determine D_{smeared} are based on the composite media theory using the approach proposed by Gérard and Marchand.[5] In their approach, the diffusion process is considered to be one-dimensional. The smeared effective diffusion coefficient $D_{e,\text{smeared}}$ is determined for the area around a crack, consisting of a parallel arrangement of a crack and the uncracked concrete, see Figure 1. Further assumptions include that the cracks are through cracks and completely saturated. $D_{e,\text{smeared}}$ is then given as Equation (6).

$$D_{e,\text{smeared}} = \frac{A_{\text{uncr}} \cdot D_{e,\text{uncr}} + A_{\text{cr}} \cdot D_{e,\text{cr}}}{A_{\text{uncr}} + A_{\text{cr}}} \quad (6)$$

where A_{uncr} and A_{cr} are the surface area of the uncracked and cracked area (m²), respectively and $D_{e,\text{uncr}}$ and $D_{e,\text{cr}}$

are the effective diffusion coefficients of the uncracked concrete and in the crack (m^2/s), respectively.

Djerbi et al.[26] performed stationary migration tests with different specimens with and without separation cracks and different crack widths to determine $D_{e,smeared}$ and $D_{e,uncr}$. Using Equation (6), the authors derived a relationship between $D_{e,cr}$ and the crack width w (μm), which appears to be independent of material effects, tortuosity, and crack roughness.

$$D_{e,cr}(w)\begin{cases} = 2e^{-11} \cdot w - 4e^{-10} & 30\,\mu m \leq w \leq 80\,\mu m \\ \approx 14e^{-10} & w > 80\,\mu m \end{cases} \quad (7)$$

Gao et al.[7] and Lu et al.[6] determined a smeared apparent diffusion coefficient referred here as $D_{smeared}$ for the whole structure based on the approach of Gérard and Marchand using the crack width w_k (mm) of bending cracks induced by service load and the maximum crack spacing $s_{r,max}$ (mm) according to Eurocode 2.[27] In their studies, effective and apparent diffusion coefficients are combined as in Equation (8) resulting in time dependent diffusion $D_{smeared}$. Both studies suggest, that Equation (8) can be used in combination with Equation (7) to determine $D_{smeared}$ as an input-parameter for the erf-solution and consequently also for the *fib* chloride model. Approaches using Equation (8) in combination with Equation (7) are later referred to as composite approach Lu/Gao.

$$D_{smeared} = D_{e,uncr} + \frac{w_k}{s_{r,max}}\left(D_{e,cr} - D_{app,uncr}\right) \quad (8)$$

Equation (8) can be transformed to Equation (9), where A_{cr} and A_{total} are the cracked and the total area of the exposed concrete surface. Approaches using Equation (9) in combination with Equation (7) are later referred to as composite approach.

$$D_{smeared} = D_{e,uncr} + \frac{A_{cr}}{A_{total}}\left(D_{e,cr} - D_{app,uncr}\right) \quad (9)$$

In the *fib* chloride model, $D_{app,c}$ from Equation (3) is a time-dependent value. Using the composite approaches, it must be decided if the uncracked concrete, represented by D_{RCM}, or $D_{smeared}$ will be expressed in a time-dependent manner. For the time-dependent composite approach, D_{RCM} and $D_{e,cr}$ are combined to get $D_{smeared}$ using the composite approach given in Equation (8) or Equation (9). Afterwards, $D_{smeared}$ is used instead of D_{RCM} in Equation (3) to determine $D_{app,c}$. The aging term and the simplified Arrhenius equation are therefore applied on both D_{RCM} and $D_{e,cr}$. In the constant composite approach, $D_{e,cr}$ is not time-dependent, which implies that the diffusion coefficient in the crack is independent of the concrete age and ambient temperature. In this case, D_{RCM} is first converted to $D_{app,c}$ and subsequently the composite approach is applied.

3.1.2 | The CIF approach to determine the smeared diffusion coefficient

For the CIF approach, chloride profiles from structural sampling or experiments are extracted at the location of a specific crack. For each chloride profile, an apparent $D_{smeared}$ can be determined by fitting the erf-solution for a specific inspection time. The CIF f_{cr} is then the ratio of $D_{smeared}$ and $D_{app,uncr}$ for uncracked concrete. Furthermore, f_{cr} can also be empirically derived as a function of the crack width w.

$$D_{smeared}(w) = f_{cr}(w) \cdot D_{app,uncr} \quad (10)$$

As an input parameter for $D_{app,uncr}$, $D_{app,c}$ from Equation (3) is used in the following. It must be highlighted, that the influence of the crack, which is represented by f_{cr} is always dependent on the time of inspection, when $D_{app,smeared}$ and $D_{app,uncr}$ were determined.

Schmiedel et al.[10] determined the influence of cracks by analyzing chloride profiles of a concrete road bridge, which was treated with deicing salts in winter. They identify f_{cr} equal to 2.3 and 2.5 for crack widths of 0.2 and 0.3 mm, respectively. Using Equation (10) with an interpolation of f_{cr} is in the following referred to as CIF Schmiedel et al.[10]

Kwon et al.[12] investigated cracked slab surfaces of a wharf structure in the marine spray area. For each crack width between 0.0 and 0.3 mm chloride profiles were obtained by drilling at the location of the crack. Based on their analysis they proposed f_{cr} as a function of crack width w (mm).

$$f_{cr}(w) = \left(31.61w^2 + 4.73w + 1\right) \text{ for } w \geq 0.1\,mm \quad (11)$$

The use of Equation (10) along with Equation (11) in this study is referred to as CIF Kwon et al.[12] Zhang et al.[13] took chloride profiles from beams, which were conditioned with 15 cycles, consisting of 1 week dry storage and 1 week immersion in NaCl-solution. Based on their experiments, they derived Equation (12) analogously to Kwon et al.[12]

$$f_{cr}(w) = \left(47.18w^2 - 8.18w + 1\right) \text{ for } w \geq 0.1\,mm \quad (12)$$

Using Equation (10) along with Equation (12) in this study is referred to as CIF Zhang et al.[13]

3.2 | Extending the convection zone to the crack depth

The use of $D_{smeared}$ in the erf-solution as diffusion coefficient D_{app} or in the *fib* chloride model as $D_{app,c}$ to account

for cracks is well established. In contrast to this procedure the approach of extending the convection zone Δx to the crack depth d_{cr} (mm), as shown in Figure 2, has never been used for the adaption of the *fib* chloride model for cracked concrete. The chloride concentration at the crack tip equals in this approach $C_{S,\Delta x}$, determined from the uncracked area of the concrete. This is a conservative approach, because the concentration of chloride ions in the cracked zone tends to decrease with the increase of crack depths and Δx is dependent on the crack width.[28] In this study, this approach is referred to as d_{cr}-adaption. Similar approaches are often used in numerical simulations,[29,30] in which the chloride concentration of the concrete surface is applied at the crack surface and the crack tip.

3.3 | Probabilistic analyses for concrete with macro-cracks

Probabilistic analyses with cracked concrete can be conducted for the cracked area or the whole concrete structure. The reliability analysis for the cracked area gives the probability of failure for the limit state of chloride-induced
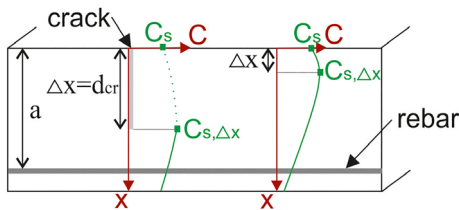

FIGURE 2 Chloride concentration C in the cracked area (left) and in the uncracked concrete (right), with the location of the convection zone $\Delta \times$

depassivation of the rebar, which is located directly underneath a certain crack. The reliability analysis for the whole structure gives a general probability of failure due to chloride-induced depassivation of rebars underneath the entire concrete cover, which includes some cracks. To account for the cracks in the concrete, either the distribution function of $D_{app,c}$ or the distribution function Δx is adapted. For this, the crack parameters w and d_{cr} should be defined as random variables.

In the first approach $D_{app,c}$ from Equation (4) is adapted to account for the cracks. For a reliability analysis focusing on the cracked area, the input to $D_{app,c}$ is the distribution function $D_{smeared}$, which can be calculated with the composite or CIF approaches. The distribution function $D_{smeared}$ is then centered at a higher value than the distribution function D_{uncr} of the uncracked concrete (see Figure 3).

If the reliability analysis is conducted for the whole structure, it must be distinguished between the composite and the CIF approaches. Using the composite approach, the distribution function of $D_{smeared}$ can be calculated for the whole structure, using Equation (8) with area ratio $\frac{w_k}{s_{r,max}}$ as input parameter. Figure 3 illustrates that $D_{smeared}$ for the whole structure peaks at a significant lower value than the distribution of $D_{smeared}$ for the cracked area, because in the latter the fraction of uncracked area considered is significantly smaller.

For the CIF approaches, a bimodal distribution $D_{uncr+smeared}$ is created, which combines fractions of the distribution functions D_{uncr} and $D_{smeared}$ (see Figure 3). A subset of the total number of samples n, which is equal to the fraction of cracked surface p_{cr} (%), are assigned with values equal to $D_{smeared}$. The rest of the samples correspond to the distribution of D_{uncr}. This approach is convenient with the Monte Carlo simulation.
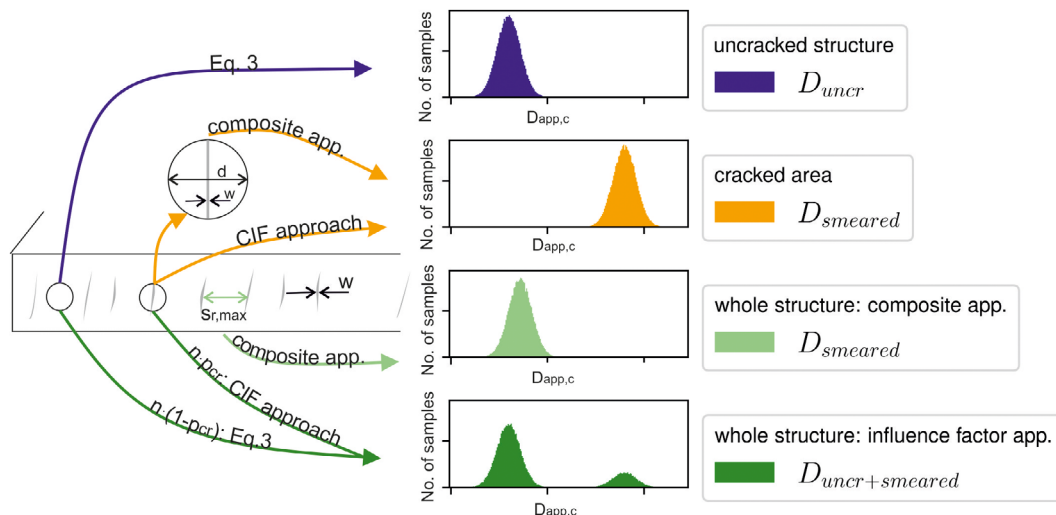

FIGURE 3 Different approaches for probabilistic reliability analysis of cracked structures with the use of $D_{smeared}$
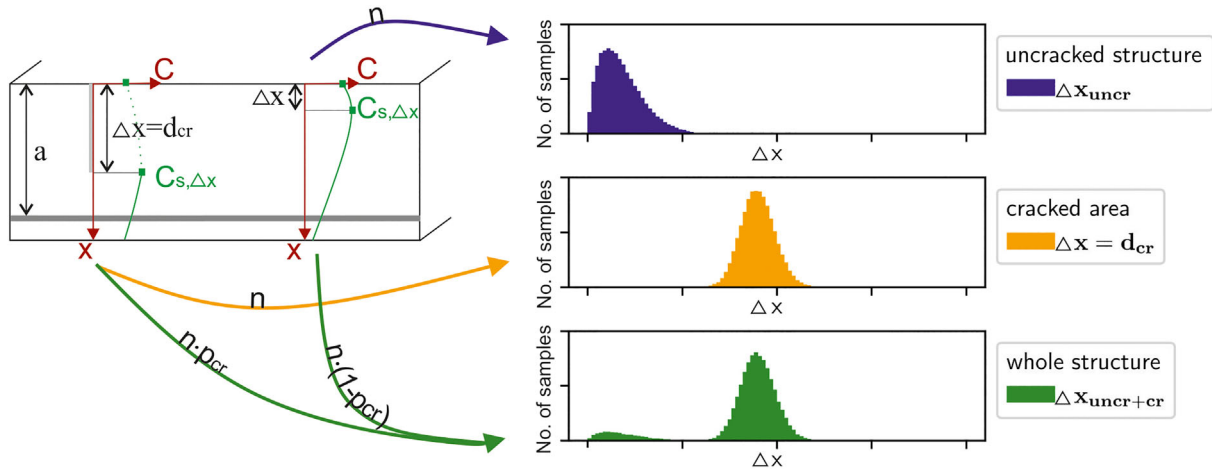
FIGURE 4 Different approaches for probabilistic reliability analysis of cracked structures with the d_{cr}-adaption

The d_{cr}-adaption is a simple approach to account for cracks in Equation (4) if the distribution function of the crack depth d_{cr} is known. The reliability analysis is carried out by increasing the convection zone Δx to d_{cr}. In the area of a crack, the distribution function of d_{cr} is used as Δx (see Figure 4). If the reliability analysis is carried out for the whole structure, p_{cr} % of the samples are assigned with values from d_{cr}. The rest is assigned with values from Δx_{uncr}. Therefore, the resulting distribution $\Delta x_{uncr+cr}$ has two maxima as shown in Figure 4. For all scenarios of the d_{cr}-adaption $D_{app,c}$ is calculated using Equation (3).

4 | CASE STUDY AND RESULTS

4.1 | Problem statement

To compare the different approaches for cracked concrete and their application to the *fib* chloride model for the service life prediction, example calculations were carried out on a defined case study. The service life prediction for both, only the cracked area and the whole structure as explained in section 3, were conducted. Subject of the case study is a reinforced concrete tubbing segment of a tunnel located in the Netherlands (Westerschelde), for which previously a service life prediction was carried out for the uncracked concrete.[31] Drilled through the soil, the exterior of the tubbing segments are located in areas exposed by chloride and largely saturated with water. A probability of failure after 50 years p_f ($t = 50$ years) of exposure is determined to be 0.74% for the uncracked concrete with a reliability index β of about 2.4. The corresponding input parameters from Reference 31 are given in Table 1 and used as it is in this study to parameterize the *fib* chloride model.

The crack width w is for all approaches assumed with a normal distribution (mean = 0.25 mm, standard deviation: 0.015 mm). The mean value of this distribution corresponds to the permissible crack width according to Eurocode 2 for the exposure class XD2.[27] The crack depth d_{cr} was conservatively assumed to cut through 90% of the concrete cover a. For the evaluation of the whole structure, it was assumed that 0.65% of the concrete surface is covered with cracks. This equals an average crack spacing $s_{r,max}$ of about 3.8 cm for a crack width of about 0.25 mm.

To predict $p_f(50)$ in the cracked area five different approaches, as discussed in section 3, are compared. To ensure that the results of these approaches are comparable $D_{smeared}$ of the composite approaches is calculated for a circular surface area (200 mm diameter) with a crack, which crosses the circular area in the middle as shown in Figure 5. This corresponds to the area investigated if a chloride profile is taken by drilling on a crack like it is done in the CIF approaches. For the sake of clarity for all approaches, considered the corresponding equations and additional parameters needed are summarized in Table 2. Each reliability analysis was carried out by a Monte Carlo simulation with 100,000 samples.

To predict the probability of failure at service life for the whole structure with 0.65% of cracked surface, six approaches were compared. All additional parameters and equations used for the model adaptations are given in Table 3. Each reliability analysis is conducted by a Monte Carlo simulation with 100,000 samples.

Finally, a parametric study was carried out for all approaches to investigate the influence of the proportion of the cracked surface p_{cr} on the probability of failure p_f. For the CIF and the composite approaches the crack width follows the same distribution as previously given

TABLE 1 Calculation example of a reinforced concrete tubbing segment from Ref. 31

Parameter (Unit)	Distribution type	Input parameter of distribution		
		Mean	Standard deviation	Bound
D_{RCM} (mm^2/year)	Normal distribution	150	30	
k_t (−)	Constant	1.0	–	
t_0 (year)	Constant	0.0767	–	
α (−)	Beta distribution	0.6	0.07	[0,1]
b_e (−)	Normal distribution	4800	700	
T_{IST} (K)	Normal distribution	282	7	
T_{ref} (K)	Constant	293	–	
$C_{s,\Delta x}$ (wt.-%/c)	Lognormal distribution	2.21	1.0	
Δx (mm)	Beta distribution	8.9	5.6	[0,50]
C_0 (wt.-%/c)	Constant	0	–	
a (mm)	Beta distribution	50	5	[0,250]
C_{crit} (wt.-%/c)	Beta distribution	0.6	0.15	[0,2]
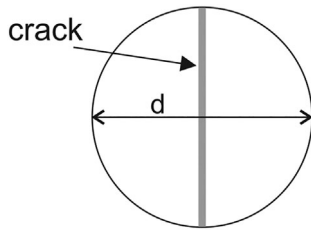
FIGURE 5 Investigated cracked area for composite approach, which corresponds to the evaluated area in the CIF approaches

in Table 3. In this scenario, p_{cr} was varied from 0% to 100%. For the d_{cr}-adaption, additionally the variation of the crack depth d_{cr}, in the range of 50%–95% of the cover depth a, is investigated. For the tubbing segments, the limit probability of failure after 50 years $p_{f,lim}(t = 50 \text{ years})$ was set at 10% for this case study, which corresponds to the recommended minimum reliability index of $\beta = 1.3$ for the limit state of chloride-induced depassivation.[1]

4.2 | Results: Cracked area

The reliability analysis for the cracked area gives the predicted probability of failure after 50 years $p_f(50)$ for a rebar, which is located directly underneath a certain crack. For the approaches considered in this study $p_f(50)$ for the same scenario ranges from 2.06% to 93.6% (see Figure 6). In comparison, $p_f(50)$ for an uncracked tubbing segment is only 0.74%. The time-dependent composite approach predicts an increase of $p_f(50)$ by the factor 3 for the cracked area, which is the lowest prediction result. The threshold probability of failure $p_{f,lim}(50)$ is

exceeded by the approach CIF Kwon et al.[12] The other CIF approaches predict up to four times smaller $p_f(50)$ than the approach CIF Kwon et al.[12] The constant composite approach predicts by far the highest $p_f(50)$, which vastly exceeds $p_{f,lim}(50)$. In comparison to the uncracked concrete, $p_f(50)$ is increased by the factor of 126.

The large variance of $p_f(50)$ for the presented approaches is due to the different $D_{smeared}$ used. In Figure 7(a,b), deterministically determined $D_{smeared}$ are shown as a function of the crack width w for 5 and 50 years, respectively. For the investigated area of the composite approaches as given in Table 2, it becomes evident that $D_{smeared}$ of all time-dependent approaches is significantly reduced with time and consequently the influence of the crack width starts to diminish. The constant composite approach, however, shows a vastly higher diffusion coefficient with increasing crack width even after 50 years, because in this approach D_{cr} is considered as constant with time.

4.3 | Results: Whole structure

The reliability analysis for the whole structure gives the probability of failure due to chloride-induced depassivation of rebars beyond the concrete cover, which includes some cracks. Figure 8 shows the results for the reliability analysis of a tubbing segment with 0.65% cracked surface. The threshold probability of failure $p_{f,lim}(50)$ of 10% is reached by the time-dependent composite approach Lu/Gao and vastly exceeded by the constant composite approach Lu/Gao. The CIF approaches Zhang et al.,[13] Kwon et al.,[12] and

TABLE 2 Additional parameters and equations needed for the different approaches to adapt $D_{app,c}$ for the cracked area

	Additional parameter	Used as $D_{app,c}$ in Equation (4)
Uncracked concrete	None	= Equation (3)
Time-dependent composite approach	$A_{total} = \pi \cdot (200/2)^2$ (mm^2) $A_{cr} = w \cdot 200$ (mm^2) $w = N(0.25, 0.015)$ (mm)	= Equation (3) with $D_{smeared}$ $D_{smeared}$ = Equation (9) $D_{e,cr}$ = Equation (7) $D_{e,uncr} = D_{RCM}$
Constant composite approach	$A_{total} = \pi (200/2)^2$ (mm^2) $A_{cr} = w \cdot 200$ (mm^2) $w = N(0.25, 0.015)$ (mm)	= $D_{smeared}$ = Equation (9) $D_{e,cr}$ = Equation (7) $D_{e,uncr}$ = Equation (3) with D_{RCM}
Time-dependent CIF[10]	$w = 0.25$ mm	= $D_{app,smeared}$ = Equation (9) $f_{cr}(w) = 2.4$ $D_{app,uncr}$ = Equation (3) with D_{RCM}
Time-dependent CIF[12]	$w = N(0.25, 0.015)$ (mm)	= $D_{app,smeared}$ = Equation (10) $f_{cr}(w)$ = Equation (11) $D_{app,uncr}$ = Equation (3) with D_{RCM}
Time-dependent CIF[13]	$w = N(0.25, 0.015)$ (mm)	= $D_{app,smeared}$ = Equation (10) $f_{cr}(w)$ = Equation (12) $D_{app,uncr}$ = Equation (3) with D_{RCM}

TABLE 3 Additional parameters and equations needed and number of samples for the different approaches to adapt Equation (4) for the whole structure

	Additional parameter	Distribution function used in Equation (4)	Number of samples
Uncracked concrete	None	$D_{app,c}$ = Equation (3) with D_{RCM} $\Delta x = Beta(8.9, 5.6, a = 0, b = 50)$	n
Time-dependent composite approach Lu/Gao for the whole structure	$w_k = N(0.25, 0.015)$ (mm) $s_{r,max} = 38.46$ mm	$D_{app,c}$ = Equation (3) $D_{smeared}$ = Equation (8) $D_{e,cr}$ = Equation (7) $D_{e,uncr} = D_{RCM}$	n
Constant composite approach Lu/Gao for the whole structure	$w_k = N(0.25, 0.015)$ (mm) $s_{r,max} = 38.46$ (mm)	$D_{app,c} = D_{smeared}$ = Equation (8) $D_{e,cr}$ = Equation (7) $D_{e,uncr}$ = Equation (3) with D_{RCM}	n

Time-dependent CIF whole structure	$p_{cr} = 0.65\%$
	$w = N(0.25, 0.015)$ (mm)
		$D_{app,c}$ = Equation (3) with D_{RCM}
		
		$D_{app,c}$ = Equation (10)
		$D_{e,uncr}$ = Equation (3) with D_{RCM}
		CIF Schmiedel (2018)[10] $f_{cr}(w) = 2.4$
		     $f_{cr}(w)$
		CIF Kwon (2009)[12] = Equation (11)
		CIF Zhang (2011)[13] $f_{cr}(w)$
		     = Equation (12)
			$n \cdot (1-p_{cr})$
			
			$n \cdot p_{cr}$

d_{cr}-adaption	$p_{cr} = 0.65\%$ $d_{cr} = 0.9 \cdot a$	$\Delta x_{uncr} = Beta(8.9, 5.6, a = 0, b = 50)$ $\Delta x_{cr} = Beta(50 \cdot 0.9, 5 \cdot 0.9, a = 0, b = 250)$	$n \cdot (1-p_{cr})$ $n \cdot p_{cr}$

Schmiedel et al.[10] predict only insignificantly higher $p_f(50)$ than for the uncracked concrete. For the same amount of cracked surface, the increase of $p_f(50)$ is less than factor 2, if the convection zone in the crack is extended to the crack depth.

4.4 | Parametric study

The parametric study is carried out to investigate the influence of the fraction of the cracked surface p_{cr} on the probability of failure $p_f(50)$. The results for the different

approaches are presented in Figure 9. If p_{cr} equals zero, $p_f(50)$ corresponds to that of the uncracked concrete. For the CIF approaches, a 100% cracked surface corresponds to the $p_f(50)$ for the cracked area. Whereas for the composite approaches, a 100% cracked surface corresponds to the $p_f(50)$ in the crack, where solely $D_{e,cr}$ is considered. As expected, an increasing p_{cr} leads to an increase of $p_f(50)$.

The results for the d_{cr}-adaption in Figure 9(a) show that $p_f(50)$ is strongly dependent on the crack depth d_{cr}. There is a linear relationship between p_{cr} and $p_f(50)$, with an increase in slope if d_{cr} increases. The parameter study also shows that $p_{f,lim}(50)$ is not reached even for deep cracks, if p_{cr} is <10%.

For the investigated range of crack width, the relationship between the p_{cr} and $p_f(50)$ is linear in the CIF approaches. Figure 9(b) shows that for the investigated

crack width in the range between 0.2 and 0.3 mm, $p_{f,lim}(50)$ is only exceeded by CIF Kwon et al.[12] In contrast, the composite approach is highly sensitive to p_{cr}, with a nonlinear relationship to $p_f(50)$. If D_{cr} is kept constant with time, the $p_f(50)$ exceeds $p_{f,lim}(50)$ starting at $p_{cr} \approx 0.01\%$, while $p_f(50)$ of the time-dependent composite approach exceeds $p_{f,lim}(50)$ starting at $p_{cr} \approx 0.65\%$ of cracked surface.

5 | LIMITATIONS OF THE EXTENSIONS FOR CONSIDERING MACRO-CRACKS IN SERVICE LIFE PREDICTIONS

The evaluation of the different *fib* chloride model extensions for the cracked concrete clearly highlights the inconsistency between them. This demonstrates the strong dependence of the probability of failure on the model extension used. To explain these inconsistences, a detailed discussion on the assumptions and limitations of the different approaches is provided in this section.

The *fib* chloride model assumes a one-dimensional chloride ingress. However, in case of cracked concrete the transport process is three-dimensional. The concentration of chloride ions in crack can quickly reach to that at concrete surface and can diffuse in perpendicular direction and starting from the crack tip into the concrete matrix.[32–34] Numerical modeling approaches on the other hand are suitable to investigate chloride ingress in cracked concrete using two-dimensional or three-dimensional geometry.[35,36] Such models can be used to systematically investigate specific crack parameters such as crack width and crack depth and also complex
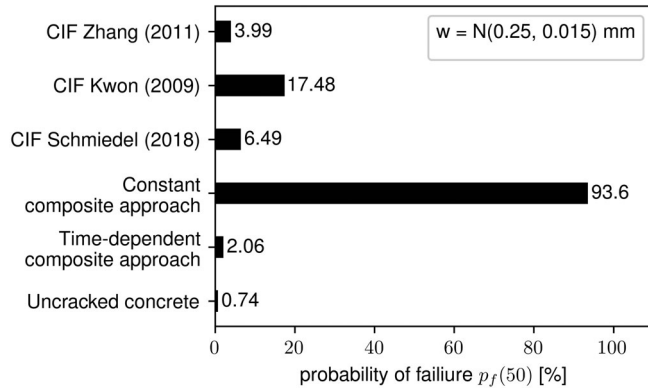
FIGURE 6 Probability of failure after 50 years $p_f(50)$ for uncracked concrete and in the cracked area, which includes a single crack ($w = N[0.25$ mm, 0.015 mm$]$)
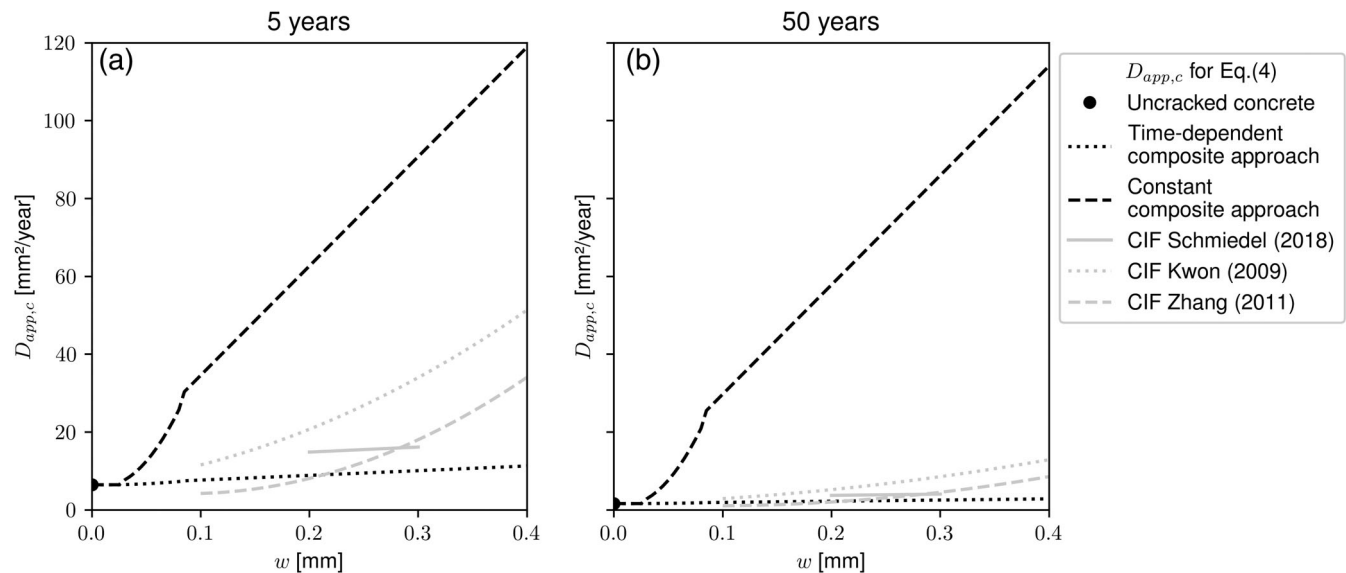
FIGURE 7 $D_{app,c}$ in dependence of the crack width w used in Equation (4) (a) after 5 years and (b) 50 years

processes, such as multi-ionic coupling effects,[37–41] can be considered in modeling. Additionally, numerical transport model can be coupled with mechanical model to simulate crack propagation and its effect on chloride transport,[39,42] which cannot be easily accounted for with analytical solutions.

For the CIF approaches, experimental investigation of chloride concentrations in cracked areas is necessary. The latter is highly sensitive to the used drill diameter. For wider drill diameters, the fraction of sound concrete in the powder sample will be higher and correspondingly, the chloride content will be lower. Furthermore, the measured chloride profiles are dependent on the crack depth and on the crack width and hence result in different values for CIFs. The latter should therefore be determined as a function of crack depth and crack width, comparable to the approach given in Reference 43. However,

the chosen drill diameters and the crack depths are hardly reported in the discussed studies.[10,12,13] Furthermore, the amount of chloride applied to the structures during the service life is not comparable in these studies. Therefore, the CIF approaches should only be used for the service life prediction of the structure, which they were determined from. In other words, these CIFs shall not be used to examine other structures.

The d_{cr}-adaption is the only approach considered in this study, which can account directly for the crack depth. The determination of the distribution function of the crack depth is, however, not straight forward. Because in practice, the crack depth of flat concrete components is usually determined by core sampling.[44] This procedure is destructive and involves a lot of effort.

For the composite approaches, the time-dependency of the diffusion coefficient has a major impact on the prediction result. Assuming that a crack is a void, ongoing hydration or chloride binding in the crack cannot be considered. Therefore, D_{cr} should not be included in Equation (3) as done in the constant time composite approach. However, crack healing can reduce the diffusion coefficient in the crack with time. For marine structures built of cementitious materials, it is reported that cracks smaller than 105 μm can heal or seal themselves autogenously and stabilize chloride penetration.[45] Therefore, the reduction of D_{cr} with time should be recognized for small cracks. For this, further systematic investigations are needed to characterize the influence of crack sealing on D_{cr} as a function of crack width and time.

The composite approach of Gérard and Marchand[5] is only derived for separating cracks where d_{cr} equals the component thickness. Bending cracks, however, have a limited d_{cr}. Experiments with bending cracks showed, that they offer a resistance to chloride penetration, which
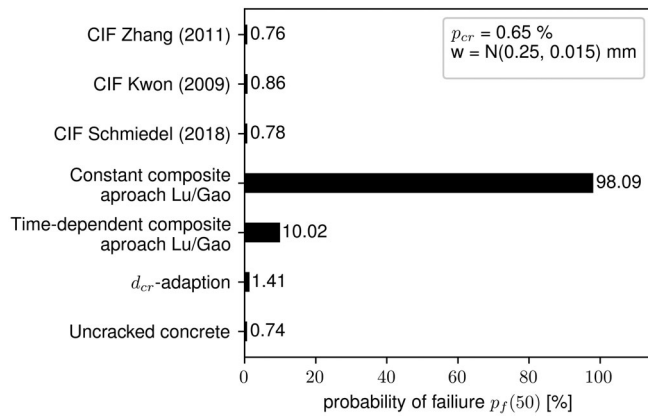

FIGURE 8 Calculated probability of failure p_f for uncracked concrete and the whole structure with 0.65% cracked surface p_{cr} for 50 years
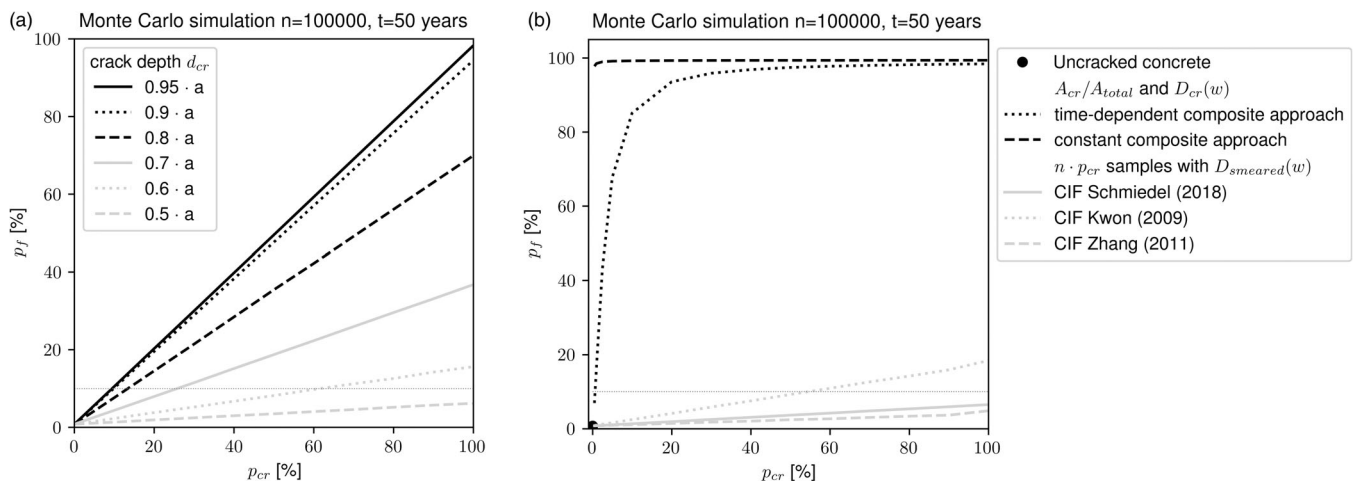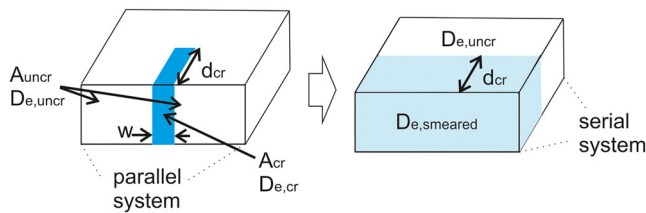

FIGURE 9 (a) Fraction of cracked surface area p_{cr} vs. probability of failure p_f for the d_{cr}-adaption for different crack depths d_{cr} (a = concrete cover). (b) p_f vs. p_{cr} for the CIF approaches and the composite approaches

FIGURE 10 Diffusion coefficients for bending cracks: Parallel system until the crack tip, serial system for whole structure

is directly proportional to d_{cr}. For such cases, additionally, a series layout can be used to obtain composite diffusion coefficients as shown in Figure 10, which has been suggested by Russo et al.[46] It must be emphasized that the determination of the diffusion coefficient concerning the composite approach with a parallel and series system is only a suitable predictor for the chloride ingress close to a crack and not for the whole structure.[47]

In addition, it must be emphasized that $D_{smeared}$ from the composite approach (Equation (9)) is not exactly same as the analytical formula from the composite media theory of Gérard and Marchand[5] (Equation (6)). Their approach can hardly be used in the context of the *fib* chloride model, because $D_{e,smeared}$ would need to be transformed to account for time dependent effects on diffusion phenomena. In addition, the *fib* chloride model needs the experimentally determined $D_{RCM,0}$ as an input-parameter, which is equivalent to $D_{app,uncr}$ for the uncracked concrete. As a consequence, the approach of Lu et al.[6] and Gao et al.[7] given in Equation (8) was adapted in this study to Equation (9). It was not possible to evaluate the influence of this discrepancy on the model results as the binding isotherm of the concrete considered in the case study is not known.

The holistic approach to consider the cracked area within the whole structure leads in the service life predictions to very low probabilities of failure. However, it is well established that cracks can cause serve damage locally[48,49] and consequently lead to the end of service of the structure. In order to classify how critical a crack for the durability of the concrete structure is, not only the crack depth and crack width but also other crack properties such as the location of the crack,[1] the crack orientation to the reinforcement,[50] and the crack spacing[47] must be considered. For modeling the chloride ingress into cracked concrete, it is important to know if the crack path is in contact with the rebar. If this is the case, the chloride transport toward the rebar is most likely not diffusion controlled, as it is assumed in Equation (4). Moreover, the limit state of depassivation due to the exceeding of the critical chloride content as described in Equation (5) will be reached within a short duration.

Therefore, to predict the durability of concrete with cracks that reach to the rebar limit states regarding the corrosion kinetics should be used. For all presented model extensions, it has therefore to be assumed, that the cracks do not reach the rebar. It has to be highlighted that the latter assumption is contradictory to Equation (8) given by Lu et al.[6] and Gao et al.[7] because the used crack width w_k (which is defined in the Eurocode 2) is the crack width at the rebar.[51]

6 | CONCLUSIONS

In this study, different approaches to extend the erf-solution (and thus also the *fib* chloride model) for the chloride ingress in cracked concrete are presented, applied, and discussed. Commonly used approaches are smeared diffusion coefficients which can be determined with the composite approach or the CIF approach. Additionally, an alternative approach has been presented in this paper, which is the adaption of the convection zone in the crack.

A case study for a cracked reinforced concrete tubbing segment exposed to chloride and largely saturated with water was carried out. For the uncracked concrete structure, the probability of failure after 50 years $p_f(50)$ was predicted to be 0.74%. For the cracked structure, $p_f(50)$ was as high as 90% if the constant composite approach, in which the diffusion coefficient in the crack remained constant over time, was used. The time-dependent composite approach and the CIF approaches predicted $p_f(50)$ between 2.06% and 17.48% in the cracked area and between 0.76% and 10.02% for the whole structure including cracks. This demonstrates the strong dependence of the predicted probability of failure on the model extension.

The modification of the one-dimensional *fib* chloride model is a rough approximation of the process, because the diffusion of chloride in cracks is three-dimensional process. The CIFs should only be used for the structures, which they were determined from. For the application of the composite approach in the *fib* chloride model, further research is required to realistically represent the time-dependence of the diffusion coefficient and the chloride binding in the crack. Adapting the convection zone, the crack depth is recognized, but the influence of a specific crack width cannot be included. Finally, it must be emphasized that the *fib* chloride model can only be extended for cracked concrete if the crack does not reach the rebar. In the case that the crack reaches to the rebar, the limit state assumption of depassivation is not applicable as the critical chloride concentration at the rebar surface can be reached within a short time period. In further

investigations, the limit state of depassivation should be replaced with the limit state of critical reinforcement section loss due to corrosion, to increase the accuracy of the service life prediction. In order to determine the service life of cracked reinforced concrete components more realistically, the three-dimensional chloride ingress should be investigated numerically (e.g., using FEM) in combination with probabilistic input parameters.

FUNDING INFORMATION

DATA AVAILABILITY STATEMENT

Data available on request from the authors.

ORCID

Annika Lidwina Schultheiß https://orcid.org/0000-0002-0036-1063

REFERENCES

1. International Federation for Structural Concrete. Model code for service life design: Bulletin no 34. 2006th ed. Lausanne: fib; 2006.
2. de Schutter G. Damage to concrete structures. Boca Raton, FL: CRC Press; 2017.
3. Richardson MG. Fundamentals of durable reinforced concrete. London: Spon; 2002.
4. Ye H, Jin N, Jin X, Fu C. Model of chloride penetration into cracked concrete subject to drying–wetting cycles. Construct Build Mater. 2012;36:259–69. https://doi.org/10.1016/j.conbuildmat.2012.05.027
5. Gérard B, Marchand J. Influence of cracking on the diffusion properties of cement-based materials. Cem Concr Res. 2000;30:37–43. https://doi.org/10.1016/S0008-8846(99)00201-X
6. Lu Z-H, Zhao Y-G, Yu Z-W, Ding F-X. Probabilistic evaluation of initiation time in RC bridge beams with load-induced cracks exposed to de-icing salts. Cem Concr Res. 2011;41:365–72. https://doi.org/10.1016/j.cemconres.2010.12.003
7. Gao Z, Liang RY, Patnaik AK. Probabilistic lifetime performance and structural capacity analysis of continuous reinforced concrete slab bridges. Int J Adv Struct Eng. 2017;9:231–45. https://doi.org/10.1007/s40091-017-0160-2
8. Park S-S, Kwon S-J, Jung SH. Analysis technique for chloride penetration in cracked concrete using equivalent diffusion and permeation. Construct Build Mater. 2012;29:183–92. https://doi.org/10.1016/j.conbuildmat.2011.09.019
9. Gowripalan N, Sirivivatnanon V, Lim CC. Chloride diffusivity of concrete cracked in flexure. Cem Concr Res. 2000;30:725–30. https://doi.org/10.1016/S0008-8846(00)00216-7
10. Schmiedel S, Vogel M, Kotan E, Müller HS. Assessment of the chloride induced depassivation of reinforcement in cracked concrete structures. In: Ye G, Yuan Y, Rodriguez CR, Zhang H, Savija B, editors. Service Life Design for Infrastructure (SLD4): Proceedings of the 4th Interna-tional Conference on Service Life Design for Infrastructures. Paris, France: RILEM; 2018).
11. Şahmaran M, Yaman İÖ. Influence of transverse crack width on reinforcement corrosion initiation and propagation in mortar beams. Can J Civ Eng. 2008;35:236–45. https://doi.org/10.1139/L07-117
12. Kwon SJ, Na UJ, Park SS, Jung SH. Service life prediction of concrete wharves with early-aged crack: probabilistic approach for chloride diffusion. Struct Saf. 2009;31:75–83. https://doi.org/10.1016/j.strusafe.2008.03.004
13. Zhang S, Lu C, Liu R. Experimental determination of chloride penetration in cracked concrete beams. Proc Eng. 2011;24:380–4. https://doi.org/10.1016/j.proeng.2011.11.2661
14. Lai J, Cai J, Chen Q-J, He A, Wei M-Y. Influence of crack width on chloride penetration in concrete subjected to alternating wetting-drying cycles. Materials (Basel, Switzerland). 2020;13:3801. https://doi.org/10.3390/ma13173801
15. Jung S-H, Ryu H-S, Karthick S, Kwon S-J. Time and crack effect on chloride diffusion for concrete with Fly ash. Int J Concr Struct Mater. 2018;12:1–10. https://doi.org/10.1186/s40069-018-0230-2
16. DuraCrete, Statistical Quantification of the Variables in the Limit State Functions: The European Union—Brite EuRam III. Contract BRPR-CT95-0132, Project BE95-1347, 2000.
17. Tang L, Nilsson L-O, Basheer PM. Resistance of Concrete to Chloride Ingress: Testing and Modelling. Hoboken: Taylor & Francis; 2010.
18. Costa A, Appleton J. Chloride penetration into concrete in marine environment—part I: Main parameters affecting chloride penetration. Mater Struct. 1999;32:252–9. https://doi.org/10.1007/BF02479594
19. Patel RA, Phung QT, Seetharam SC, Perko J, Jacques D, Maes N, et al. Diffusivity of saturated ordinary Portland cement-based materials: a critical review of experimental and analytical modelling approaches. Cem Concr Res. 2016;90:52–72. https://doi.org/10.1016/j.cemconres.2016.09.015
20. Jasielec JJ, Stec J, Szyszkiewicz-Warzecha K, Łagosz A, Deja J, Lewenstam A, et al. Effective and apparent diffusion coefficients of chloride ions and chloride binding kinetics parameters in mortars: non-stationary diffusion-reaction model and the inverse problem. Materials (Basel, Switzerland). 2020;13:5522. https://doi.org/10.3390/ma13235522
21. Lay S. Probabilistische Abschätzung der Lebensdauer von tausalzexponierten Stahlbetonbauwerken: Baustein eines Systems zum Lebenszyklusmanagement von Stahlbetonbauwerken. Dissertation, München. 2006.
22. Vu KAT. Corrosion-induced cracking and spatial time-dependent reliability analysis of reinforced concrete structures. Dissertation, The University of Newcastle. 2003.
23. Crank J. The Mathematics of Diffusion. 2nd ed. Oxford: Oxford University Press; 1975.
24. Gehlen C, von Greve-Dierfeld SM, Gulikers J, Helland S, Rahim A. Benchmarking of Deemed-to-Satisfy Provisions in Standards: Durability of Reinforced Concrete Structures Exposed to Chlorides; State-of-the-Art Report. Lausanne, Switzerland: Fédération Internationale du Béton; 2015.
25. Šomodíková M, Strauss A, Zambon I, Teplý B. Quantification of parameters for modeling of chloride ion ingress into

concrete. Struct Concr. 2019;20:519–36. https://doi.org/10.1002/suco.201800049

26. Djerbi A, Bonnet S, Khelidj A, Baroghel-Bouny V. Influence of traversing crack on chloride diffusion into concrete. Cem Concr Res. 2008;38:877–83. https://doi.org/10.1016/j.cemconres.2007.10.007

27. DIN Deutsches Institut für Normung e. V. Eurocode 2: Bemessung und Konstruktion von Stahlbeton- und Spannbetontragwerken – Teil 1–1: Allgemeine Bemessungsregeln und Regeln für den Hochbau; Deutsche Fassung EN 1992-1-1:2004 + AC. 2004th ed. Berlin: Beuth Verlag GmbH; 2010.

28. Ye H. Chloride-induced steel corrosion in concrete under service loads. Singapore: Springer Singapore Pte. Limited; 2020.

29. Sosdean C, Marsavina L, de Schutter G. Experimental and numerical determination of the chloride penetration in cracked mortar specimens. Eur J Environ Civ Eng. 2016;20:231–49. https://doi.org/10.1080/19648189.2015.1035802

30. Bentz DP, Garboczi EJ, Lu Y, Martys N, Sakulich AR, Weiss WJ. Modeling of the influence of transverse cracking on chloride penetration into concrete. Cem Concr Compos. 2013;38:65–74. https://doi.org/10.1016/j.cemconcomp.2013.03.003

31. Gehlen C. Probabilistische Lebensdauerbemessung von Stahlbetonbauwerken: Zuverlässigkeitsbetrachtungen zur wirksamen Vermeidung von Bewehrungskorrosion. Dissertation, Beuth, Aachen. 2000.

32. Geiker M, Danner T, Michel A, Belda Revert A, Linderoth O, Hornbostel K. 25 years of field exposure of pre-cracked concrete beams; combined impact of spacers and cracks on reinforcement corrosion. Constr Build Mater. 2021;286:122801. https://doi.org/10.1016/j.conbuildmat.2021.122801

33. Weiss J, Couch J, Pease B, Laugesen P, Geiker M. Influence of mechanically induced cracking on chloride ingress in concrete. J Mater Civ Eng. 2017;29:4017128. https://doi.org/10.1061/(ASCE)MT.1943-5533.0001922

34. Li Y, Chen X, Jin L, Zhang R. Experimental and numerical study on chloride transmission in cracked concrete. Construct Build Mater. 2016;127:425–35. https://doi.org/10.1016/j.conbuildmat.2016.10.044

35. Peng J, Hu S, Zhang J, Cai CS, Li L. Influence of cracks on chloride diffusivity in concrete: a five-phase mesoscale model approach. Construct Build Mater. 2019;197:587–96. https://doi.org/10.1016/j.conbuildmat.2018.11.208

36. Li G, Yao F, Liu P, Yan C. Long-term carbonation resistance of concrete under initial high-temperature curing. Mater Struct. 2016;49:2799–806. https://doi.org/10.1617/s11527-015-0686-3

37. Liu Q, Easterbrook D, Yang J, Li L. A three-phase, multi-component ionic transport model for simulation of chloride penetration in concrete. Eng Struct. 2015;86:122–33. https://doi.org/10.1016/j.engstruct.2014.12.043

38. Meng Z, Liu Q, She W, Cai Y, Yang J, Farjad Iqbal M. Electro-chemical deposition method for load-induced crack repair of reinforced concrete structures: a numerical study. Eng Struct 246. 2021;246:112903. https://doi.org/10.1016/j.engstruct.2021.112903

39. Meng Z, Liu Q, Xia J, Cai Y, Zhu X, Zhou Y, et al. Mechanical–transport–chemical modeling of electrochemical repair methods for corrosion-induced cracking in marine concrete. Comput Aided Civ Inf Eng. 2022. https://doi.org/10.1111/mice.12827

40. Liu Q, Yang J, Xia J, Easterbrook D, Li L, Lu X. A numerical study on chloride migration in cracked concrete using multi-component ionic transport models. Comput Mater Sci. 2015;99:396–416. https://doi.org/10.1016/j.commatsci.2015.01.013

41. Zhang C, Chen W, Mu S, Šavija B, Liu Q. Numerical investigation of external sulfate attack and its effect on chloride binding and diffusion in concrete. Construct Build Mater. 2021;285:122806. https://doi.org/10.1016/j.conbuildmat.2021.122806

42. Liu Q, Hu Z, Wang X, Zhao H, Qian K, Li L, et al. Numerical study on cracking and its effect on chloride transport in concrete subjected to external load. Construct Build Mater. 2022;325:126797. https://doi.org/10.1016/j.conbuildmat.2022.126797

43. de Schutter G. Quantification of the influence of cracks in concrete structures on carbonation and chloride penetration. Mag Concr Res. 1999;51:427–35. https://doi.org/10.1680/macr.1999.51.6.427

44. Günter M, Ruckenbrod C. Risse – Erkennen, Einordnen und Untersuchen. In: Haist M, editor. Beherrschung von Rissen in Beton 7. Symposium Baustoffe und Bauwerkserhaltung. Karlsruhe: KIT Scientific Publishing; 2010. p. 41–66.

45. Maes M, Snoeck D, de Belie N. Chloride penetration in cracked mortar and the influence of autogenous crack healing. Construct Build Mater. 2016;115:114–24. https://doi.org/10.1016/j.conbuildmat.2016.03.180

46. Russo N, Gastaldi M, Marras P, Schiavi L, Strini A, Lollini F. Effects of load-induced micro-cracks on chloride penetration resistance in different types of concrete. Mater Struct. 2020;53:1–14. https://doi.org/10.1617/s11527-020-01580-y

47. Wang X-Y, Zhang L-N. Simulation of chloride diffusion in cracked concrete with different crack patterns. Adv Mater Sci Eng. 2016;2016:1–11. https://doi.org/10.1155/2016/1075452

48. Michel A, Sørensen HE, Geiker MR. 5 years of in situ reinforcement corrosion monitoring in the splash and submerged zone of a cracked concrete element. Construct Build Mater. 2021;285:122923. https://doi.org/10.1016/j.conbuildmat.2021.122923

49. Ji Y, Hu Y, Zhang L, Bao Z. Laboratory studies on influence of transverse cracking on chloride-induced corrosion rate in concrete. Cem Concrete Compos. 2016;69:28–37. https://doi.org/10.1016/j.cemconcomp.2015.12.006

50. Shaikh FUA. Effect of cracking on corrosion of steel in concrete. Int J Concr Struct Mater. 2018;12:3. https://doi.org/10.1186/s40069-018-0234-y

51. Zilch K, Zehetmaier G. Bemessung im konstruktiven Betonbau: Nach DIN 1045–1 (Fassung 2008) und EN 1992-1-1 (Eurocode 2). 2nd ed. Berlin: Springer; 2010.

AUTHOR BIOGRAPHIES

Annika Lidwina Schultheiß Institute of Building Materials and Concrete Structures (IMB), Karlsruhe Institute of Technology (KIT) and Materials Testing and Research Institute Karlsruhe (MPA), Karlsruhe Institute of Technology (KIT), DE-76131, Karlsruhe, Germany annika.schultheiss@kit.edu

Ravi A. Patel

Institute of Building Materials and Concrete Structures (IMB), Karlsruhe Institute of Technology (KIT), DE-76131, Karlsruhe, Germany Materials Testing and Research Institute Karlsruhe (MPA), Karlsruhe Institute of Technology (KIT), DE-76131, Karlsruhe, Germany

ravi.patel@kit.edu

Michael Vogel

Institute of Building Materials and Concrete Structures (IMB), Karlsruhe Institute of Technology (KIT), DE-76131, Karlsruhe, Germany Materials Testing and Research Institute Karlsruhe (MPA), Karlsruhe Institute of Technology (KIT), DE-76131, Karlsruhe, Germany

michael.vogel@kit.edu

Frank Dehn

Institute of Building Materials and Concrete Structures (IMB), Karlsruhe Institute of Technology (KIT), DE-76131, Karlsruhe, Germany Materials Testing and Research Institute Karlsruhe (MPA), Karlsruhe Institute of Technology (KIT), DE-76131, Karlsruhe, Germany

frank.dehn@kit.edu